TIME DOMAIN IDENTIFICATION OF FRAMES UNDER EARTHQUAKE LOADINGS

By Chin-Hsiung Loh,[1] Member, ASCE, Chi-Ying Lin,[2] and Chih-Chieh Huang[3]

ABSTRACT: The purpose of this paper is to examine the adaptive identification method and the nonlinear system identification technique through numerical simulation on seismic response of building structures. For the identification of a time-variant system and a system with an abrupt change of modal parameters, two parameter adaptation algorithms in recursive identification methods are discussed: recursive least square algorithm with constant trace and adaptive fading Kalman filter method. Based on the equivalent linear model, the time-variant model parameters can be identified. The tracking ability on the identification of a time-variant system is discussed. For the identification of the nonlinear system, the forward including algorithm and the neural network training algorithm were used to estimate the modal parameter of the nonlinear autoregressive moving average model, and the accuracy on the predicted output of nonlinear model identification was discussed.

INTRODUCTION

Identification is the process of developing an accurate mathematical model for a system, given a set of inputs and corresponding output measurements. In earthquake engineering, field problems involving the identification of structural systems exhibiting inelastic restoring forces are widely encountered. For the purpose of damage assessment and possible retrofit of the structure during strong ground excitation, it is desirable to identify severity as well as location of the damage based on the input-output measurements. The use of system identification techniques for nondestructive and damage evaluations is an important and challenging problem. Recent efforts to apply formal system identification concepts to the problem of detection of changes in structural parameters include the work of Shinozuka et al. (1982), Masri et al. (1982), Naike and Yao (1986, 1987), and Agbabian et al. (1991). In general, identification methods can be categorized as those in the time domain and the frequency domain. In the frequency domain method, modal quantities such as natural frequencies, damping ratios, and mode shapes are identified. The reverse dynamic system of spectral analysis (Bendat et al. 1992) and the generalized frequency response function estimated from the nonlinear autoregressive moving average (NARMA) model (Billings et al. 1990) were applied in nonlinear system identification. On the other hand, in the time domain method, system parameters were determined from observational data sampled in time. It is necessary to identify the time variation of system dynamic characteristics from time domain approach if the properties of the structural system change with time under strong external loading condition. Tracking of time-varying phenomena and nonlinear behavior of dynamic system became an important problem in the area of structural system identification.

Numerous techniques are available for the recursive estimation to time-varying parameters. These methods involve some kind of forgetting (i.e., discounting of old data). The following equation is considered a system described by the linear regression:

$$y(t) = \boldsymbol{\varphi}^T(t)\boldsymbol{\theta}_0 + e(t) \tag{1}$$

where the regression vector $\boldsymbol{\varphi}^T(t)$ = known function of the information variable at time $t - 1$; $e(t)$ = sequence of independent random variables with $E[e(t)] = 0$ and $E[e^2(t)] = \sigma^2$; and $\boldsymbol{\theta}_0$ = vector of unknown parameters. A standard algorithm for calculating $\boldsymbol{\theta}_0$ is the recursive least squares (RLS) method, which can be written (Ljung and Söderström 1983)

$$\hat{\boldsymbol{\theta}}(t) = \hat{\boldsymbol{\theta}}(t - 1) + \mathbf{P}(t)\boldsymbol{\varphi}(t)[y(t) - \boldsymbol{\varphi}^T(t)\hat{\boldsymbol{\theta}}(t - 1] \tag{2}$$

$$\mathbf{P}^{-1}(t) = \mathbf{P}^{-1}(t - 1) + \boldsymbol{\varphi}(t)\boldsymbol{\varphi}^T(t) \tag{3a}$$

in which

$$\mathbf{P}^{-1}(t) = \sum_{i=1}^{t} \boldsymbol{\varphi}(i - 1)\boldsymbol{\varphi}^T(i - 1) \tag{3b}$$

From (3), it can be seen that if $\{\varphi\}$ sufficiently exists, the elements of $\mathbf{P}$ converge to zero, and $\hat{\boldsymbol{\theta}}$ becomes constant. Hence, in the case of time-varying parameters [$\boldsymbol{\theta}_0 = \boldsymbol{\theta}(t)$], the traditional RLS method is unsuitable to detect the time-varying model dynamic characteristics owing to the loss of tracking capability. A different recursive identification method must be studied to increase the tracking ability.

The easiest way to increase the tracking ability in the recursive formula for the inverse of the adaptation gain $\mathbf{P}^{-1}(t)$ given by (3) is generalized by introducing two weighting sequences $\lambda_1(t)$ and $\lambda_2(t)$, as indicated below

$$\mathbf{P}(t + 1)^{-1} = \lambda_1(t)\mathbf{P}(t)^{-1} + \lambda_2(t)\boldsymbol{\varphi}(t)\boldsymbol{\varphi}(t)^T \quad \text{and} \quad 0 < \lambda_1(t) \leq 1;$$

$$0 < \lambda_2(t) \leq 2 \tag{4}$$

where $\lambda_1(t)$ tends to increase the adaptation gain; and $\lambda_2(t)$ tends to decrease the adaptation gain. A certain number of choices for $\lambda_1(t)$ and $\lambda_2(t)$, such as decreasing gain, constant forgetting factor, and variable forgetting factor have been used. These types of profiles are recommended for the identification of stationary systems or for the identification of a slowly time-varying system because they avoid a too rapid decrease of the adaptation gain. For the identification of nonstationary data and time-varying systems, the constant trace method can be applied. In this case, $\lambda_1(t)$ and $\lambda_2(t)$ are automatically chosen at each time step to ensure a constant trace of the gain matrix (constant sum of the diagonal terms of $\mathbf{P}$). This way $\mathbf{P}$ cannot be getting smaller and smaller so as to lose the tracking ability.

Unlike the model shown in (1), the system equation of motion can also be represented in the state-space formulation, where stiffness matrix [$\mathbf{K}$] and damping matrix [$\mathbf{C}$] of the dynamic system become the unknown system parameters. For

[1]Prof., Dept. of Civ. Engrg., Nat. Taiwan Univ., Taipei, Taiwan; and Dir. of Nat. Ctr. for Res. on Earthquake Engrg., Taipei, Taiwan.

[2]Grad. Student, Dept. of Civ. Engrg., Nat. Taiwan Univ., Taipei, Taiwan.

[3]Res. Asst., Dept. of Civ. Engrg., Nat. Taiwan Univ., Taipei, Taiwan.

Note. Special Editor: Roger Ghanem. Discussion open until December 1, 2000. To extend the closing date one month, a written request must be filed with the ASCE Manager of Journals. The manuscript for this paper was submitted for review and possible publication on February 25, 2000. This paper is part of the ***Journal of Engineering Mechanics***, Vol. 126, No. 7, July, 2000. ©ASCE, ISSN 0733-9399/00/0007-0693–0703/ $8.00 + $.50 per page. Paper No. 22238.

this identification problem, the sequential regressional analysis (Caravani et al. 1977) and the normal Kalman filter technique (Hoshiya and Saito 1984) can be used to estimate the model parameters. This filter estimation depends highly on the past data, and the system model degrades the measurement information from the distant past. To overcome this problem, the filter should be capable of eliminating the effect of old data from a current estimate. Due to the complex nature of civil infrastructure and noise-polluted measurement, it becomes a challenging task to model the current structure for identification. Application of an adaptive H_∞-filter to identify the time-variant model parameters is one promising tool in identification (Sato and Qi 1998).

The purpose of this paper is to make a summary report on the use of system identification techniques to estimate the dynamic characteristics of building frames from seismic response data. The identification methods include adaptive fading Kalman filter (AFKF) technique and neural modeling of the NARMA model. The effect of model inaccuracy in identification is also discussed.

DISCUSSION OF MODEL INACCURACY IN STRUCTURAL IDENTIFICATION

In structural system identification, different mathematical models will induce different explanations on the result of identification even with the same set of input/output data. The modal inaccuracy in structural system identification can be categorized into two items: (1) The uncertainty due to nonlinear model; and (2) the completeness of model description (or exact description). Selecting the exact model becomes one of the important issues for identification.

Test of Nonlinearity

Many structural systems exhibit linear behavior at low levels of excitation, which allows estimation of modal parameters using a constant parameter linear system. Unfortunately, as the level of excitation increases, the system may not continue to respond in a linear fashion. The successful development of identification procedures for a nonlinear system depends on the selection of nonlinear terms. The criterion to judge whether the system is linear or nonlinear should be adapted before identification. An index is suggested to compare the difference between the frequency response function (FRF) and the Hilbert transform of FRF (Loh and Duh 1996). The index (ID) is defined as follows:

$$ID(\%) = \left\{\frac{H_v - G_v}{G_v}\right\} \cdot 100 \tag{5a}$$

where

$$H_v = \int_{\omega_1}^{\omega_n} H(\omega)\, d\omega; \quad G_v = \int_{\omega_1}^{\omega_2} G(\omega)\, d\omega \tag{5b}$$

and $G(\omega)$ = amplitude of FRF between input and output signals; and $H(\omega)$ = amplitude of Hilbert transformation of $G(\omega)$. For a linear system, the response at any time does not depend on the input, and the Hilbert transform of a linear system is equal to the FRF of that system's $G(\omega)$. If the Hilbert transform does not equal the FRF, then the system is nonlinear. Application of the Hilbert transform can provide a measure of system nonlinearity from which the nonlinear model can be used to present the nonlinear system and reduce the model selection between linear and nonlinear system.

Identification of Mode Shapes

Relating the completeness on the description of the structural model, the selected model must reflect the actual dynamic characteristics of the structure. Generally, the shear-type model is the most common simple model for solving the inverse problem. But this shear-type model cannot be used for all kinds of building structures. For example, on the identified mode shape of a building structure, it is assumed that the mode shape $\phi_i(x)$ of any building frame with or without walls may be estimated by a combination of shear and flexural modes

$$\phi_i(x) = \alpha_i \eta_i(x) + \beta_i \psi_i(x), \quad i = 1 \sim N \tag{6}$$

where $\eta_i(x)$ and $\psi_i(x)$ = flexural mode shape and shear mode shape of ith mode, respectively; and α_i and β_i = contribution factors from a different model. In most of the structural identification of building frames, the shear-type mathematical model was used, which may not be correct in most cases. It is possible to examine the significant error to be induced due to the incomplete description of the structural model.

The structural response data of the shaking table test of a 5-story 1/2-scale steel frame, with 3 × 2 m dimensions in-plane and 1.3 m for each story, was used in this study. Fig. 1 shows the side view of the test structure in the longitudinal direction. The first and second natural frequency modes of the structure longitudinally are 1.40 and 4.524 Hz, respectively. The ground motion data collected at the Japan Kobe Marine Meteorological Observatory (JKM) station for the Kobe earthquake (Jan. 17, 1994) was used as input motion. Four different levels of input peak ground acceleration (PGA) were assigned: 16, 24, 40, and 60% of Kobe earthquake ground motion at the JKM station. Fig. 2 shows the comparison on the roof acceleration among different levels of excitation. Based on (5), the frequency response function $G(\omega)$ was estimated between input motion and roof response and its Hilbert transform for different levels of input excitation. Table 1 shows the index of nonlinearity detection. Fig. 3 shows the comparison of the amplitude of the estimated $G(\omega)$ and the Hilbert transform of $G(\omega)$, $H\{G(\omega)\}$. It is found that a larger index $ID(\%)$ value was calculated from the structural response data subjected to a higher intensity level of excitation [i.e., excitation from 60% of Kobe earthquake will have $ID(\%)$ = 13.66%, which is almost six times larger than the result calculated from 16% level

Benchmark Model	Period (sec)	
	Dir-2m	Dir-3m
1st Mode	0.467	0.699
2nd Mode	0.143	0.216

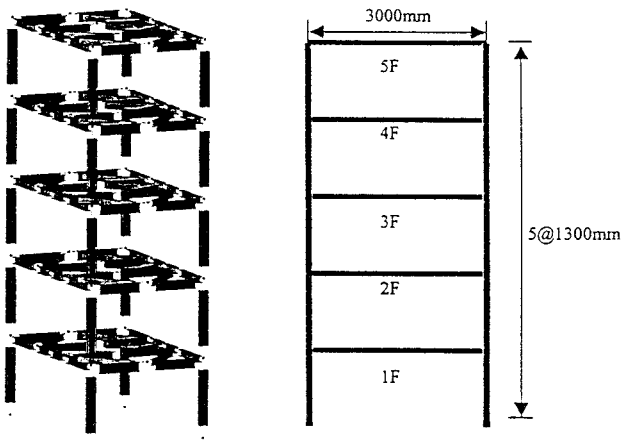

FIG. 1. Model of 5-Story Steel Frame; Natural Period of System and Side View of Frame Is Also Shown

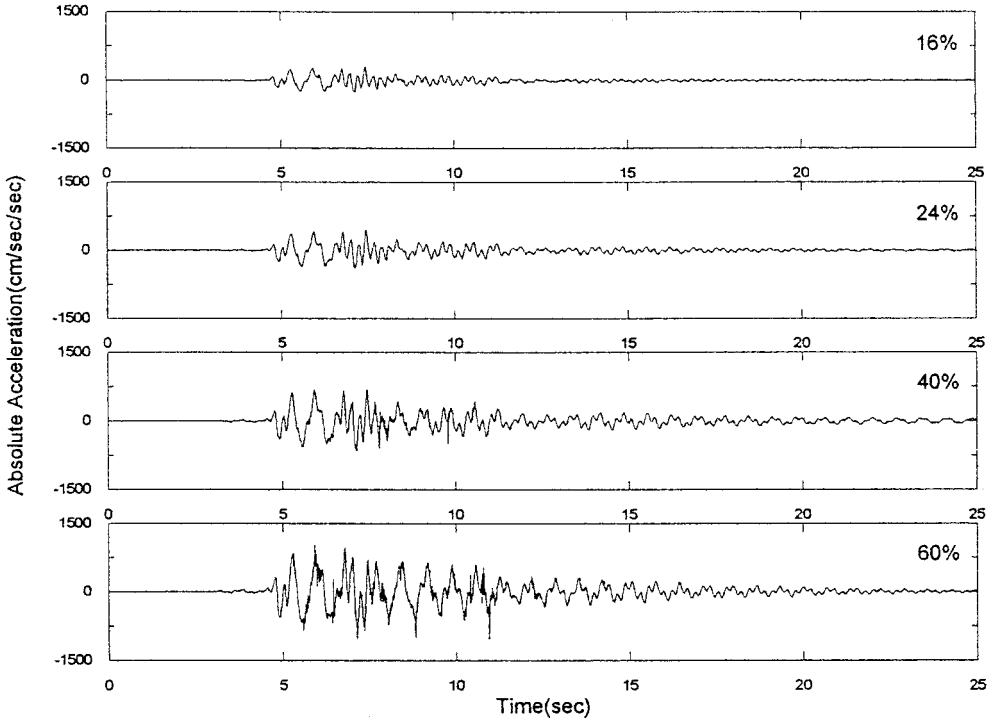

FIG. 2. Plot of Roof Acceleration Response from Shaking Table Test of Benchmark Model; Comparison on Roof Response for Four Different Intensity Levels of Excitation

TABLE 1. Plot of *ID* ($n = 0$) Index for Different Levels of Excitation

Excitiation level (Kobe) (1)	Error (%) (2)
16%	2.1
24%	2.21
40%	9.36
60%	13.66

of excitation]. This indicated that the steel frame did not reflect linear behavior under the stronger ground motion excitation.

The other issue to be considered in system identification is the selection of mathematical model accurately. Based on the response measurement, the estimation of mode shapes from the test data is shown in Fig. 4. The identified mode shapes were fitted to the linear combination of shear type and flexure type mode shapes, as indicated in (6). Table 2 shows the estimated coefficients α_i and β_i for the first and second modes. It was found that the contribution of flexure type mode shape to the estimated mode shape is also important under different levels of excitation, particularly for the second mode shape.

Mathematical Model for Identification

To avoid using only the shear-beam-type model, the floor rotation model was developed for structural identification. Based on the element stiffness matrix with the consideration of joint rotation, as shown in Fig. 5, the stiffness matrix is derived. To include the joint rotation in modeling the system, the system dynamic equation can be expressed

$$[M]\{\ddot{x}\} + [C]\{\dot{x}\} + [K]\{x\} = -[M]\{1\}\ddot{x}_g(t) \qquad (7a)$$

where

$$\{x\}^T = \langle v_1, v_2, \ldots, v_5, \theta_1, \theta_2, \ldots, \theta_5 \rangle^T \qquad (7b)$$

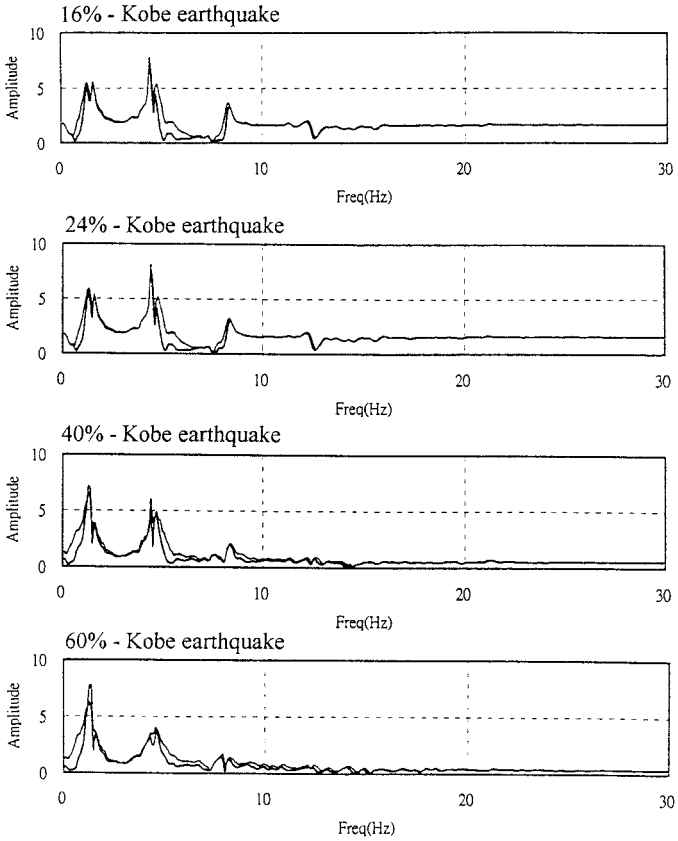

FIG. 3. Comparison between System FRF and Hilbert Transform of FRF from Experimental Data of Different Intensity Levels of Excitation

$v_i(t)$ = horizontal displacement of ith floor; and θ_i = floor beam-column joint rotation. Based on the element stiffness (shown in Fig. 5), the stiffness matrix of the building can be expressed

$$[K] = \begin{bmatrix} 2k_1 & -k_1 & 0 & 0 & 0 & 0 & k_2 & 0 & 0 & 0 \\ -k_1 & 2k_1 & -k_1 & 0 & 0 & -k_2 & 0 & k_2 & 0 & 0 \\ 0 & -k_1 & 2k_1 & -k_1 & 0 & 0 & -k_2 & 0 & k_2 & 0 \\ 0 & 0 & -k_1 & 2k_1 & -k_1 & 0 & 0 & -k_2 & 0 & k_2 \\ 0 & 0 & 0 & -k_1 & k_1 & 0 & 0 & 0 & -k_2 & -k_2 \end{bmatrix} \quad (7c)$$

where

$$k_1 = \frac{12EI}{L^3}; \quad k_2 = \frac{6EI}{L^2}$$

It is assumed that the EI value for each floor remains the same. The modified stiffness matrix includes horizontal shear stiffness as well as floor rotational stiffness. In building response

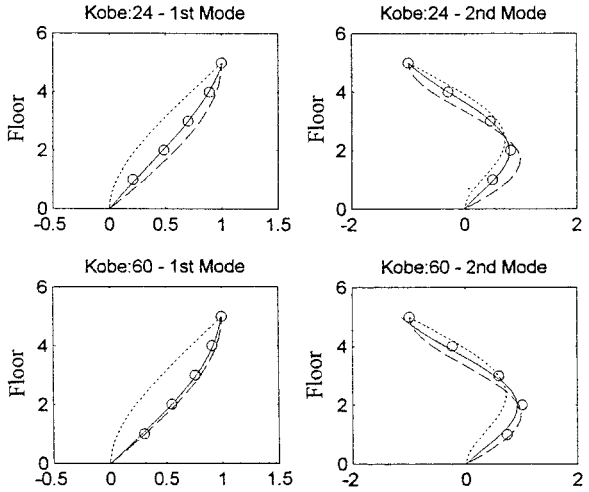

FIG. 4. Identified First and Second Mode Shapes from Test Building with Different Intensity Levels of Excitation (24% and 60% Levels of Excitation of Kobe Earthquake) (Dotted Line and Dashed Line Are Mode Shape of Shear Type and Flexural Type, Respectively)

TABLE 2. Estimated Mode Shape Contribution Factor for Flexure Type α_i and Shear Type β_i from Data of Different Excitation Levels

Excitation level (1)	First Mode		Second Mode	
	α_1 (2)	β_1 (3)	α_2 (4)	β_2 (5)
16%	0.1660	0.6748	0.2757	0.4448
24%	01617	0.6838	0.2867	0.4349
40%	0.0376	0.9109	0.3548	0.4760
60%	0.0448	0.9021	0.3020	0.5444

measurement, the floor rotation θ_i cannot be directly measured but it can be obtained through the derivative of horizontal deformation. Assuming that the horizontal displacement $v(z, t)$ is a function of building height z and time t, the floor tation can then be obtained through regression analysis from the measurement of horizontal direction at each floor. Then the joint rotation can be expressed

$$\theta_i(z_i, t) = \left.\frac{dv(z, t)}{dz}\right|_{z=z_i} \quad (8)$$

where $v(z, t)$ = horizontal displacement of the building at height z; and $\theta_i(t)$ is evaluated at $z = z_i$. Of course, it is assumed that floor responses (including velocity, displacement, and rotation) can be measured or calculated for identification. Sequential regression analysis was applied to identify k_1, k_2 and also the damping matrix **C**. Table 3 shows the estimated modal parameters from the data of different levels of excitation. Fig. 6 shows the comparison between the estimated floor velocity and the recorded velocity at each floor for input motions with 24 and 60% levels of Kobe earthquake excitation. As shown in Table 4, it is clear that the RMS error of the response is much smaller if the shear-type model with floor rotation was considered. The RMS error is larger at the lower floor level (particularly for larger amplitude of excitation) because of the nonlinear response at that floor level. The current linear model cannot fit the data very well.

TIME DOMAIN SYSTEM IDENTIFICATION

System identification techniques can be divided into two groups. One group of techniques uses the nonparametric approach to determine the input-output map using the least-squares method. The input-output map is characterized by a system model that may not have any explicit physical meaning. Another group of techniques uses the parametric approach to determine the parameters of a system model. The parameters may represent physical quantities such as the structural rigidity, mass inertia, etc.

System Realization Algorithm

Based on the mathematical framework, the system realization using information matrix (SRIM) is established (Juang 1997). The SRIM is derived using the state-space discrete-time linear equation to form a data correlation matrix for system identification. Based on the discrete-time autoregressive with exogenous input model, the following matrix equality can be developed:

$$\alpha Y_p(k) = \beta U_p(k) \quad (9a)$$

where

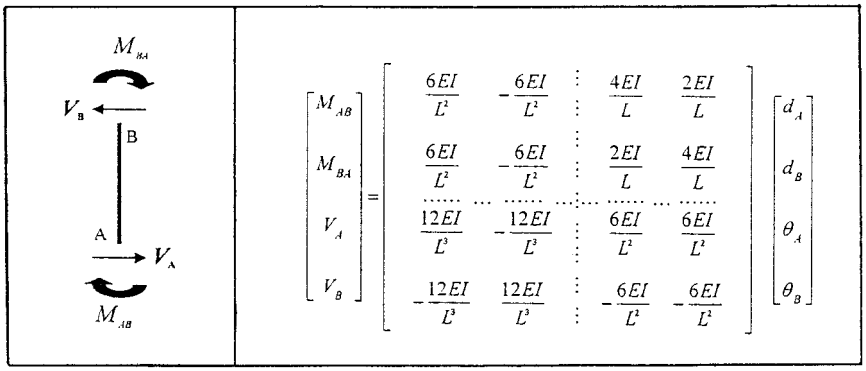

FIG. 5. Element Stiffness Matrix Considering Bending and Shear Forces

TABLE 3. Estimated Model Parameters[a] from Shaking Table Test of Benchmark Model

Parameters (1)	PGA Level (Kobe Earthquake) 16% (2)	24% (3)	40% (4)	60% (5)
k_1	7915.95	8349.09	8706.28	7534.05
k_2	3397.84	3664.77	3867.66	3199.18
c_1	57.73	65.28	68.15	52.74
c_2	32.13	37.90	38.80	12.48
c_3	34.60	41.93	40.95	12.55
c_4	37.97	39.51	39.04	20.68
c_5	41.04	41.02	39.70	25.94

[a]Shear-type model with floor rotation.

$$\alpha = [\alpha_0 \quad \alpha_1 \quad \cdots \quad \alpha_{p-1}]; \quad \beta = [\beta_0 \quad \beta_1 \quad \cdots \quad \beta_{p-1}];$$

$$Y_p(k) = \begin{bmatrix} y(k) & y(k+1) & \cdots & y(k+N-1) \\ y(k+1) & y(k+2) & \cdots & y(k+N) \\ \vdots & \vdots & \ddots & \vdots \\ y(k+p-1) & y(k+p) & \ddots & y(k+p+N+2) \end{bmatrix};$$

$$U_p(k) = \begin{bmatrix} u(k) & u(k+1) & \cdots & u(k+N-1) \\ u(k+1) & u(k+2) & \cdots & u(k+N) \\ \vdots & \vdots & \ddots & \vdots \\ u(k+p-1) & u(k+p) & \ddots & u(k+p+N+2) \end{bmatrix} \tag{9b}$$

Postmultiplying (9*a*) by $U_p^T(k)$, one can obtain the correlation matrix

$$\alpha[R_{yy} - R_{yu}R_{uu}^{-1}R_{uy}^T] = 0 \tag{10a}$$

or

$$\alpha R_{hh} = 0_{m\times pm} \tag{10b}$$

One may take a singular value decomposition to factor the matrix $\mathbf{R}_{hh}$, and then the state matrix **A** can be obtained. With the computed matrix **A**, the system dynamic characteristics can be estimated. For example, consider the seismic response of the 5-story steel frame. Based on the seismic response data collected from the 8% excitation level of the Kobe earthquake excitation, the above-mentioned SRIM method was applied to identify the natural frequency and damping ratio of the system. Fig. 7 shows the comparison of the recorded and estimated first floor acceleration response. Good estimations can be obtained. The identified first and second natural frequency modes of the steel frame are 1.397 and 4.520 Hz, and the damping ratios are 1.71 and 0.18%, respectively. This method can be applied to the estimated dynamic characteristics of the linear system using limited measurements.

Linearly Parameterized Estimator

Problems involving the inelastic restoring forces are widely encountered in the earthquake engineering field. Numerous methods for the identification of nonlinear systems have been developed in the past decade (Diaz and Desrochers 1988; Safac 1989; Stry and Moak 1992; Sato and Qi 1998). Most methods fall into one of the following categories:

- Describe the nonlinear system using a linear model.
- Obtain a graphical representation of the nonlinear term, then find an analytical model for the nonlinearity.
- Represent the nonlinear system in an expansion series and obtain the respective coefficients by using a regression estimation.

Among the methods that linearize the nonlinear system is the on-line identification using equivalent nonstationary but

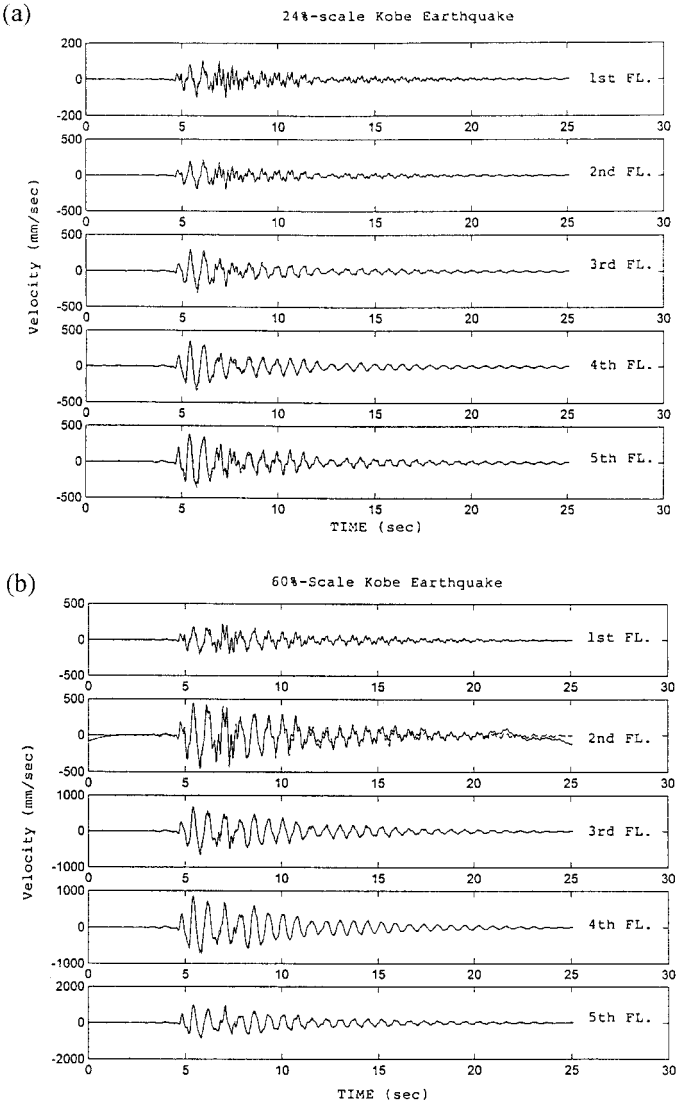

FIG. 6. Comparison on Floor Velocity Responses between Identified and Experimental Results for: (a) System Subjected to 24%-Scale of Kobe Earthquake Ground Motion; (b) System Subjected to 60%-Scale of Kobe Earthquake Ground Motion

TABLE 4. RMS Error between Estimated and Recorded Data

Benchmark model (1)	RMS ERROR: Displacement Response Model A (2)	Displacement Response Model B (3)	Velocity Response Model A (4)	Velocity Response Model B (5)
(a) 24% Excitation Level of Kobe Earthquake				
First floor	0.318	0.064	0.541	0.258
Second floor	0.292	0.034	0.501	0.137
Third floor	0.269	0.025	0.308	0.079
Fourth floor	0.265	0.022	0.248	0.062
Fifth floor	0.272	0.022	0.298	0.076
(b) 60% Excitation Level of Kobe Earthquake				
First floor	0.226	0.035	0.496	0.145
Second floor	0.201	0.016	0.407	0.146
Third floor	0.182	0.012	0.202	0.036
Fourth floor	0.174	0.011	0.151	0.031
Fifth floor	0.176	0.011	0.191	0.042

Note: Model A is a shear type model, and Model B is a shear type model with floor rotation.

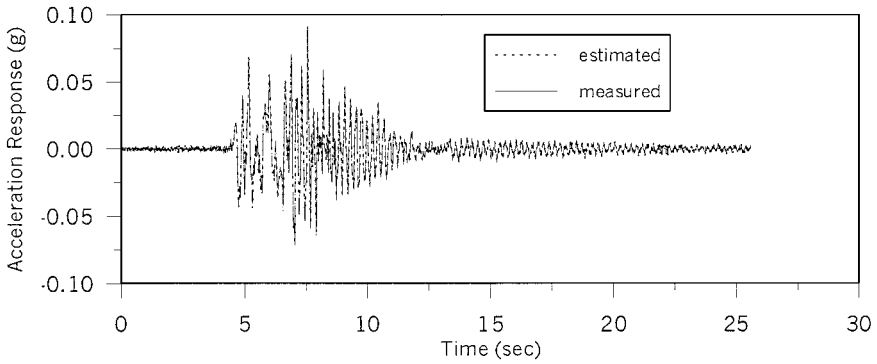

FIG. 7. Comparison on Acceleration Response of First Floor between Recorded and Estimated Results Using SRIM Method

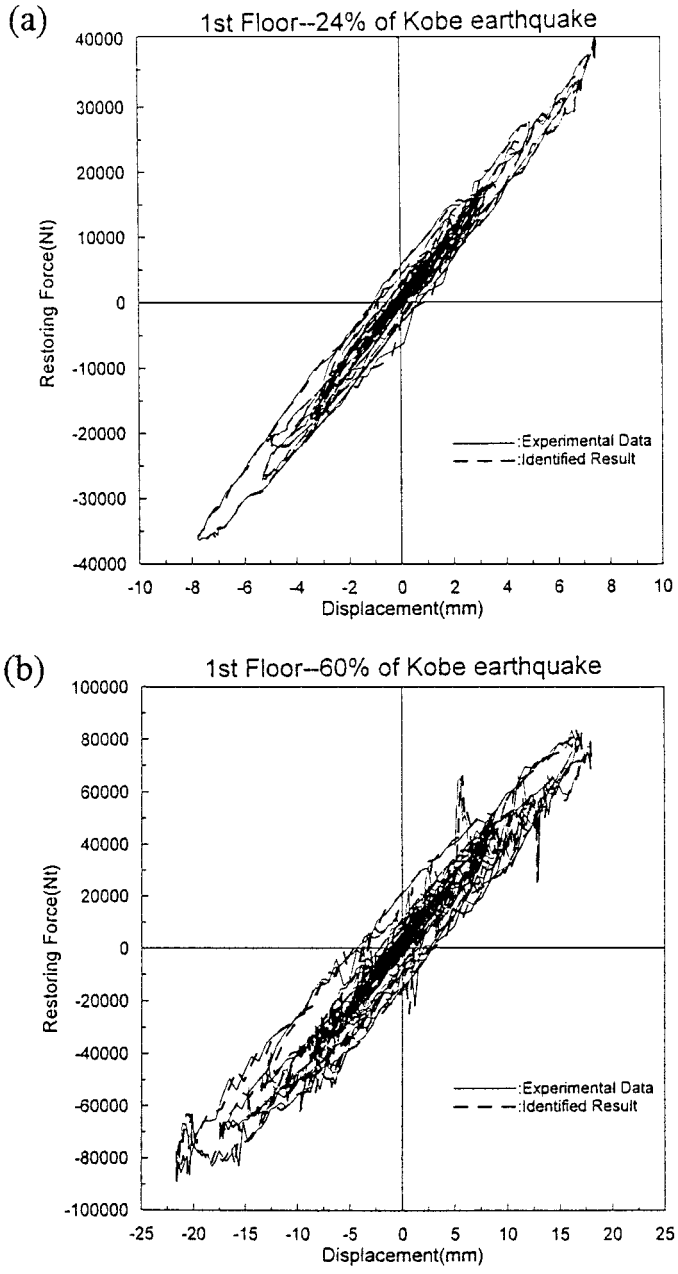

FIG. 8. Comparison between Experimental and Identified First Floor Restoring Force Diagram of Benchmark Model Results of: (a) 24% Level of Kobe Earthquake Excitation; (b) 60% Level of Kobe Earthquake Excitation

linear structural parameters (Loh and Lin 1996). From the practical point of view, the autoregressive with exogenous input system described by the following model:

$$y(t) = \sum_{j=1}^{r} a_j(t)y(t-j) + \sum_{j=1}^{p} b_j(t)u(t-j) + n(t) \qquad (11)$$

is the most common model to be discussed. To detect the nonlinear characteristics using a linear model, a variable forgetting factor algorithm can be used in which the forgetting factors were determined based on the memory length (Ioan 1990). However, if the model parameters can be parameterized linearly with respect to the coefficients, then it is desirable to use a linear parameterized estimation for the on-line estimation of the hysteretic behavior. The RLS methods can be applied directly (Chassiakos and Masri 1994). Consider a nonlinear hysteretic system with restoring force represented as the Bouc-Wen model. Assuming that $n = 2$, the restoring force $z(t)$ can be expressed

$$\dot{z}(t) = \left(\frac{1}{\eta}\right)[A\dot{x} - a_1 v(\beta|\dot{x}|z + \gamma\dot{x}|z|) - a_2 v(\beta|\dot{x}||z|z + \gamma\dot{x}|z|^2)] \qquad (12)$$

One can discretize the differential equation and express it as follows:

$$z(k) = z(k-1) + \theta_0\dot{x}(k-1) - \theta_1|\dot{x}(k-1)|z(k-1) + \theta_2\dot{x}(k-1)|z(k-1)| - \theta_3|\dot{x}(k-1)||z(k-1)|z(k-1) + \theta_4\dot{x}(k-1)|z(k-1)|^2 \qquad (13)$$

where

$$\theta_0 = A\left(\frac{1}{\eta}\right)\Delta t; \quad \theta_1 = -a_1\left(\frac{1}{\eta}\right)v\beta\Delta t; \quad \theta_2 = a_1\left(\frac{1}{\eta}\right)v\gamma\Delta t;$$

$$\theta_3 = -a_2\left(\frac{1}{\eta}\right)v\beta\Delta t; \quad \theta_4 = a_2\left(\frac{1}{\eta}\right)v\gamma\Delta t$$

Using the data collected from the shaking table test of a 5-story steel frame, one can identify the modal parameters of the restoring force using the Kalman filter technique. Fig. 8 shows the comparison of the restoring force for different set of data. Good agreement between identified and experimental results were observed. The identified parameters $\theta_i (i = 0-4)$ using $n = 2$ are shown in Table 5.

AFKF Method

Unlike the model shown in (9), the system equation of motion can also be represented in state-space formulation. The Kalman filter approach can be applied to estimate the modal parameters (Sato and Takei 1997). The equation describing the

TABLE 5. Identified Model Parameters of Bouc-Wen Inelastic Model for $n = 2$

Excitation levels (%) (1)	$n = 2$				
	θ_0 (2)	θ_1 (3)	θ_2 (4)	θ_3 (5)	θ_4 (6)
8	29.7664	5.4455×10^{-4}	-5.043×10^{-4}	-6.114×10^{-8}	-4.637×10^{-9}
16	26.9575	1.8445×10^{-4}	-5.148×10^{-6}	-1.159×10^{-8}	-8.283×10^{-9}
24	26.1114	3.98×10^{-5}	3.851×10^{-5}	-2.085×10^{-9}	-3.936×10^{-9}
40	24.4941	-2.514×10^{-5}	1.06×10^{-4}	-4.71×10^{-10}	-2.81×10^{-9}
60	24.8119	5.614×10^{-5}	-8.573×10^{-5}	-3.84×10^{-9}	9.66×10^{-10}

optimal estimator can be expressed as follows (the normal Kalman filter):

$$\hat{x}(k|k-1) = \Phi(k, k-1)\hat{x}(k-1) \tag{14a}$$

$$\hat{\mathbf{x}}(k) = \hat{x}(k|k-1) + K(k)[\mathbf{y}(k) - \mathbf{H}(k)\hat{x}(k|k-1)] \tag{14b}$$

where

$$K(k) = F(k|k-1)H^T(k)[\mathbf{H}(k)F(k|k-1)H^T(k) + R(k)]^{-1} \tag{15a}$$

$$F(k+1|k) = \mathbf{\Phi}(k+1, k)F(k)\Phi^T(k + 1, k) + G(k)Q(k)G^T(k) \tag{15b}$$

$$F(k) = [1 - K(k)\mathbf{H}(k)]F(k|k-1) \tag{15c}$$

where $\hat{\mathbf{x}}(k) = n \times 1$ state vector; $\mathbf{y}(k) = m \times 1$ measurement vector; $\mathbf{\Phi}(k+1, k)$ and $\mathbf{H}(k)$ = state transition matrix and observation matrix, respectively. The $\hat{\mathbf{x}}(k)$ is an augmented state vector with unknown parameters. Because filter estimation depends highly on past data and the system model degrades the measurement information from the distant past, the heavy reliance on past data may cause the state estimation to diverge. To overcome this problem, the filter should be capable of eliminating the effect of old data from a current estimate.

In developing the AFKF algorithm, the addition of the forgetting factor $\lambda(k)$ in the time propagating error covariance matrix is suggested (Xia et al. 1994)

$$F(k+1|k) = \lambda(k+1)\mathbf{\Phi}(k+1, k)F(k)\Phi^T(k+1, k) + G(k)Q(k)G^T(k) \tag{16}$$

with $\lambda(k+1) \geq 1.0$. The optimal filter asks the residual $Z(k)$ [defined as $Z(k) = \mathbf{y}(k) - \mathbf{H}(k)\hat{x}(k|k-1)$] to be a white noise sequence; that is, the sequence of residuals is uncorrelated when an optimum gain is used, $C_j(k) = E[Z(k+j)Z^T(k)] = 0$. In other words, if a forgetting factor can be chosen so that $C_j(k)$ becomes zero, then the Kalman gain $K(k)$ is optimal. Substituting (15) into $C_j(k) = E[Z(k+j)Z^T(k)]$ and if the gain is optimal, the following equation is satisfied:

$$F(k|k-1)H^T(k) - K(k)C_0(k) = 0 \tag{17}$$

where $K(k)$ = estimated Kalman filter. Eq. (17) is the basis for the development of the adaptive filtering algorithm. A residual matrix is then defined

$$\mathbf{S}(k) = F(k|k-1)H^T(k) - K(k)C_0(k) \tag{18}$$

Hence the forgetting factor $\lambda(k)$ in (16) should be chosen to minimize $g(\lambda, k)$, where

$$g(\lambda, k) = \frac{1}{2}\sum_i \sum_j S_{ij}^2(k) \tag{19}$$

The optimality of the Kalman filter can be judged by the scalar function $g(\lambda, k)$, and $S_{ij}(k)$ is the (i, j)th element of $\mathbf{S}(k)$. The physical meaning of optimal forgetting factor is that, for unknown drifts and process changes, the adaptive fading algorithm compensates the increasing estimation error by choosing larger forgetting factors.

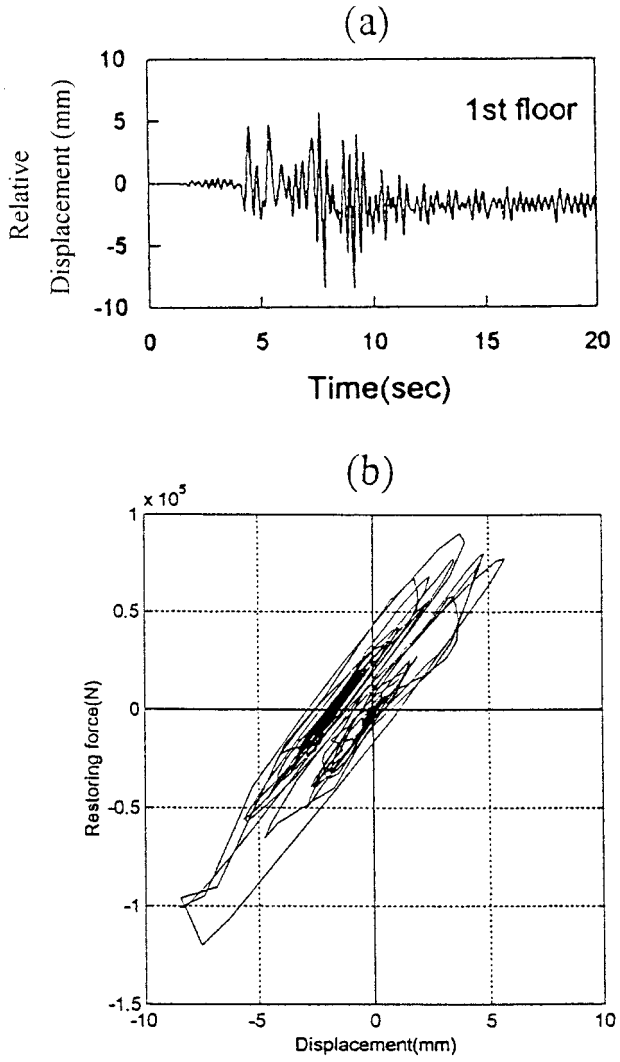

FIG. 9. (a) Simulated First Floor Displacement (Relative to Ground); (b) Plot of First Floor Restoring Force Diagram to Show Hysteresis Behavior of Building

Consider a 5-story steel frame where the fundamental period of the structure is 0.278 s. Structural response data was obtained by using the DRAIN-2DX program to simulate the response of the structure subjected to Kobe earthquake excitation (data were recorded at JKM station and PGA value was normalized to $0.5g$). Fig. 9 shows the calculated first floor relative displacement and the restoring force of the first floor. The AFKF technique was used to identify the time-varying stiffness and damping of the local system (first floor). From the response, it is clear that permanent deformation was observed in the displacement of the first floor, as shown in Fig. 10. The restoring force diagram was shifted to one side of the diagram after a few cycles of responses. Because the permanent deformation occurred within a very short time period

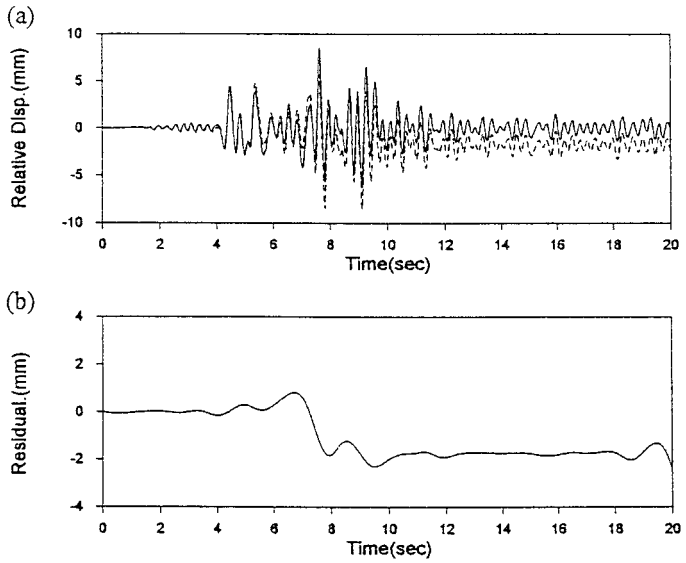

FIG. 10. (a) Relative Displacement of First Floor (Dotted Line: Simulated Response, Solid Line: Removal of Permanent Deformation); (b) Identified Permanent Deformation from Huang et al.'s Modal Decomposition Method (1998)

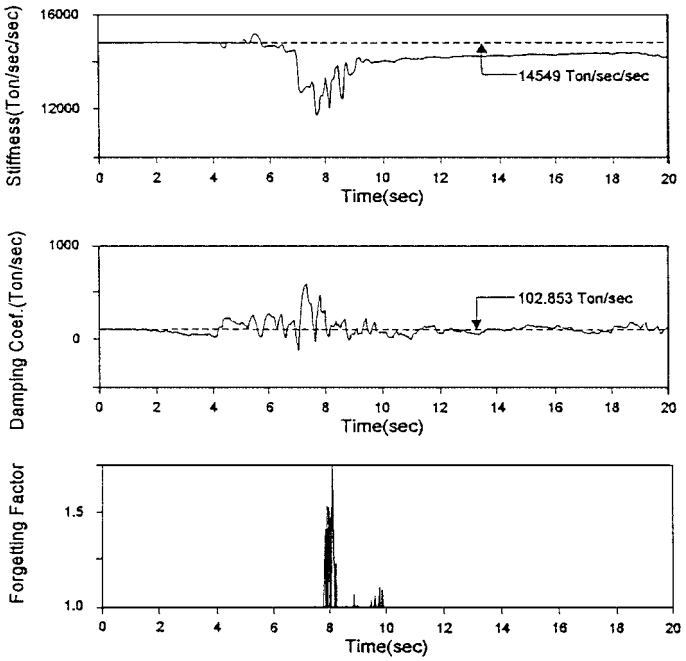

FIG. 11. Identified Time-Varying Stiffness and Damping of First Floor Using AFKF Technique; Forgetting Factor in AFKF Is Also Shown

(1–2 s), it is necessary to remove this permanent deformation before performing the identification. The empirical mode decomposition method (Huang et al. 1998) can be applied to remove the permanent offset of floor response. After removing the permanent displacement, the time-varying stiffness can then be identified using the AFKF algorithm. Fig. 11 shows the estimated time-variant stiffness and damping of the first floor. The forgetting factor is also shown. This example describes the nonlinear system using a linear model to detect the time-varying modal parameters.

NARMA METHODOLOGY WITH TRAINING OF NEURAL NETWORKS

As discussed in the previous section, one of the methods in the identification of a nonlinear system is to find an analytical model to represent the nonlinearity. The nonlinear functions of damping force and restoring force of a real nonlinear system are generally not known. However, by expanding the system output in terms of past input and output using a NARMA model, a representation for a wide class of nonlinear systems can be obtained (Billings and Tsang 1989; Chen and Billings 1989; Billings et al. 1990). A single input single output system takes the form (NARMA)

$$y(t) = F^l[y(t-1), \ldots, y(t-n_y), u(t), \ldots, u(t-n_u), \varepsilon(t-1), \ldots, \varepsilon(t-n_\varepsilon)] \quad (20)$$

where $y(t)$ and $u(t)$ represent the measured output and input, respectively; $\varepsilon(t)$ = prediction error; and $F^l[\ ]$ is some nonlinear function. To determine the nonlinear function, the analysis involved fitting linear models to various orders (n_u, n_y) and delays (d) and computing the loss functions (sum of squared errors) of the fitted models using the least square algorithm with $l = 1$. Fitting a linear model as a first step almost always indicates to the investigator a suitable choice for n_u and n_y. This is valuable information because it defines a smaller search space for the nonlinear terms. In the model equation of (18), one can also incorporate the velocity term ($\dot{y}(t)$) to represent the nonlinear damping. Theoretical works performed by Funahashi (1989) proved that neural networks can approximate any continuous function even with a single hidden layer. A hyperbolic tangent sigmoid function can be chosen as the nonlinear transfer function at each neuron and the Levenberg-Marquardt back-propagation algorithm is used to train the network. This therefore gives the theoretical basis for modeling nonlinear systems by a neural network. Neural-network-based approach is regarded as a kind of nonparametric method.

Because the network was used as a model of unknown nonlinearity of prediction of the system's responses to various excitations, artificial neural networks can be used for the identification of the internal (restoring) forces of some typical nonlinear structural systems. By using $\mathbf{x}$ and $\dot{\mathbf{x}}$ as input signals, $\ddot{\mathbf{x}}$ as output signals), the training procedure will use the nonlinear function mapping capability to avoid this nonlinear term selection (nonlinear model determination) problem. If the system exhibits hysteretic behavior, it is important to include the lagged information in the model to represent this energy-dissipating phenomenon.

Unlike the identification of restoring forces, the network-based approach is also used for the detection of changes in the characteristics of structure-unknown systems. For example, consider the 5-story structure again. Measured responses are considered as an acceleration at each floor, and the mathematical description of these responses is not clear. By putting an acceleration at the first and third floors as input signals and a second floor acceleration as an output signal, hidden layer activation functions are either linear or nonlinear; the relation may still be established (if it exists) between these responses through the training process and can be used as a tool for structural health monitoring. The underlying idea can be explained in the following procedures: (1) Establish the neural networks from the response of structures subjected to low level excitation, and train the system to ''learn'' the behavior of a ''healthy'' structure; and (2) based on these established networks, put the current measured responses from the monitoring structure into the trained network for safety evaluation. The deviation from the network output and true structural response could be an indicator of the current condition of the structure. A large deviation indicates that the damage has occurred in the structure or the structural behavior has changed. Similar ideas were found by Masri et al. (1996). This technique will be used in this study to identify the change of RMS

error values of a bridge structure when subjected to earthquake excitation.

Example 1

Consider an example of a nonlinear Duffing equation with $\ddot{u}_g(t)$ as input motion

$$mx + cx + k_1x + k_2x^3 = -m\ddot{u}_g(t) \tag{21}$$

with $m = 1$; $c = 3.77$; $k_1 = 355.3$; $k_2 = 700$; and subjected to input motion $\ddot{u}_g(t)$ (El Centro earthquake ground motion normalized the PGA value to $0.196g$). In the beginning, the initial analysis involved finding linear models of various orders. Table 6 lists the identified terms [Model A is obtained from Loh and Duh (1996)]. The RMS value of two different models is also shown. Table 7 shows the linear model loss function for the Duffing system and for a case of displacement output. By using the displacement output (Table 7) the delays ($n_y = n_{\dot{y}} = n_u = 3$) are selected as a starting point for identification. By using the velocity output (Table 8), the delays (n_y, $n_{\dot{y}}$, and n_u) are chosen as either 3 or 4 (models A, B, C, and D are modeled with one neuron and models E and F are modeled with 5 and 7 neurons, respectively). It is found that the RMS error by choosing the velocity signal as output is much larger than by choosing the displacement signal as input. Based on the identified model, the trained network is fed with different input data (such as different PGA levels of the Kobe earthquake, etc.), then the outputs from the network and the system are compared to each other. Table 9 also shows the RMS error of the matching outputs from the data of velocity output. Three training cases are identified: Case No. 1, (El Centro earthquake, PGA = $0.22g$), Case No. 2 (El Centro earthquake, PGA = $0.196g$), and Case No. 6 (Kobe earthquake, PGA = $0.25g$). The results show that the neural network training approach provides an alternative method to identify the nonlinear function of the NARMA model and the modal parameters.

TABLE 6. Identified Model Parameters Via Regression Analysis for Models A and B

Term (1)	Model A (2)	Model B (3)
(a) Displacement Output		
$U(k-1)$	0.0102	−0.0002
$U(k-2)$	0.0002	0.0003
$U(k-3)$	—	−0.0002
$Y'(k-1)$	—	0.0485
$Y'(k-2)$	—	−0.0302
$Y'(k-3)$	—	−0.0115
$Y(k-1)$	−3.6212	−0.1610
$Y(k-2)$	0.9295	2.9974
$Y(k-3)$	—	−1.8289
$Y(k-1)^3$	−7.2676	—
RMS error	0.0111	0.0065
(b) Velocity Output		
$U(k-1)$	−0.0211	−0.0241
$U(k-2)$	0.0330	0.0526
$U(k-3)$	−0.0147	−0.0326
$U(k-4)$	—	0.0014
$Y'(k-1)$	4.0157	2.4928
$Y'(k-2)$	−2.3608	−8.7476
$Y'(k-3)$	−0.9811	−3.1670
$Y'(k-4)$	—	−0.0842
$Y(k-1)$	−145.3399	85.4600
$Y(k-2)$	307.1823	330.5600
$Y(k-3)$	−161.4377	−395.7173
$Y(k-4)$	—	−20.0025
RMS error	0.0483	0.0479

Example 2

Consider the 5-story steel frame (as shown in Fig. 1). The network was designed to model the second floor response from the upper and lower responses of that floor. The input infor-

TABLE 7. Linear Model Loss Function for Duffing System (Delays $n_y = n_{\dot{y}} = n_u = 3$ Are Selected as Starting Point for System Identification for Case of Displacement Output)

Delay	$n_{\dot{y}}$					
n_y	0	1	2	3	4	5
0		0.9221	0.4970	0.4786	0.4415	0.4241
1	0.3889	0.0461	0.0234	0.0199	0.0180	0.0141
2	0.0883	0.0215	0.0187	0.0182	0.0163	0.0135
3	0.0444	0.0183	0.0181	0.0180	0.0162	0.0135
4	0.0362	0.0166	0.0166	0.0154	0.0138	0.0126
5	0.0344	0.0161	0.0156	0.0123	0.0123	0.0120

Delay	Delay	n_u					
n_y	$n_{\dot{y}}$	0	1	2	3	4	5
3	3	0.0180	0.0157	0.0068	0.0065*	0.0064	0.0064
3	4	0.0162	0.0140	0.0068	0.0065	0.0064	0.0064
3	5	0.0135	0.0126	0.0068	0.0064	0.0064	0.0064
4	3	0.0154	0.0133	0.0067	0.0064	0.0064	0.0064
4	4	0.0138	0.0114	0.0067	0.0064	0.0064	0.0064
4	5	0.0126	0.0112	0.0066	0.0064	0.0064	0.0064
5	3	0.0123	0.0113	0.0067	0.0064	0.0064	0.0064
5	4	0.0123	0.0111	0.0066	0.0064	0.0064	0.0064
5	5	0.0120	0.0111	0.0066	0.0064	0.0064	0.0064

	Linear	NonLinear n_h			
n_y $n_{\dot{y}}$ n_u	1	1	3	5	7
3	0.0065	0.0065	0.0064*	0.0062	0.0062

Note: * indicates RMS error from different training cases, and remaining values indicate RMS error from prediction.

TABLE 8. Six Different NARMA Models Identified from Velocity Output Data

Model (1)	Equation (2)
A	$\dot{y}(k) = \sum_{i=1}^{3} a_i \dot{y}(k-i) + \sum_{j=1}^{3} b_j y(k-j) + \sum_{s=1}^{3} c_s u(k-s)$
B	$\dot{y}(k) = \sum_{i=1}^{4} a_i \dot{y}(k-i) + \sum_{j=1}^{4} b_j y(k-j) + \sum_{s=1}^{4} c_s u(k-s)$
C	$\dot{y}(k) = w_1 \times f\left(\sum_{i=1}^{3} a_i \dot{y}(k-i) + \sum_{j=1}^{3} b_j y(k-j) + \sum_{s=1}^{3} c_s u(k-s)\right)$
D	$\dot{y}(k) = w_1 \times f\left(\sum_{i=1}^{4} a_i \dot{y}(k-i) + \sum_{j=1}^{4} b_j y(k-j) + \sum_{s=1}^{4} c_s u(k-s)\right)$
E	$\dot{y}(k) = \sum_{m=1}^{5}\left(w_m \times f\left(\sum_{i=1}^{4} a_{mi} \dot{y}(k-i) + \sum_{j=1}^{4} b_{mj} y(k-j) + \sum_{s=1}^{4} c_{ms} u(k-s)\right)\right)$
F	$\dot{y}(k) = \sum_{m=1}^{7}\left(w_m \times f\left(\sum_{i=1}^{4} a_{mi} \dot{y}(k-i) + \sum_{j=1}^{4} b_{mj} y(k-j) + \sum_{s=1}^{4} c_{ms} u(k-s)\right)\right)$

mation to the network is chosen to be the first and third floor current values of acceleration response and immediate history of these quantities. From the ''loss function table,'' the identified maximum value of delay time for acceleration at the first and third floors are $n_{a1} = n_{a3} = 4$ and 8 for Models A and B, respectively. From Table 10 it is shown that the linear model with 8-step lagged information (Model B) is superior to that with 4-step (Model A). The identified nonlinear function is shown in Table 11. The results show that if the network is trained with data from low level excitation, the network cannot produce the same level of prediction error to the structure under high level excitation, or vice versa. In addition to Models A and B, a nonlinear model can also be trained (Model C). The results show that if the model was trained with data from the low level excitation, then it cannot predict the response from high level excitation. On the contrary, if the network trained with the data from high level excitation, then it can predict the response of low level excitation.

CONCLUSIONS

The purpose of this paper is to present a systematic method for the identification of either a time-variant system or a nonlinear dynamic system. To detect the time-variant system or a system with an abrupt change of modal parameters, the AFKF provides an efficient method for the system identification. For the identification of a nonlinear system, either a linearly parameterized estimator or an extended Kalman filter technique can be applied if the nonlinear hysteretic model is known. On the contrary, if the nonlinear hysteretic model is unknown, the NARMA methodology with neural network design can be used

TABLE 9. RMS Error (Using Velocity Signal as Output) Based on Six Different Models (A, B, C, D, E, and F) and Trained with Three Different Cases (1, 2, and 6)

	Training case					
	Model A			Model B		
Testing case	1	2	6	1	2	6
El_ns_220gal	0.0433*	0.0433	0.0627	0.0431*	0.0434	0.0795
El_ns_196gal	0.0483	0.0483*	0.0689	0.0480	0.0479*	0.0875
El_ns_100gal	0.0526	0.0526	0.0746	0.0525	0.0525	0.0951
El_ns_50gal	0.0546	0.0545	0.0772	0.0545	0.0545	0.0984
El_ns_10gal	0.0552	0.0551	0.0780	0.0551	0.0551	0.0994
Kobs_ns_250gal	0.0279	0.0278	0.0142*	0.0282	0.0299	0.0122*
Kobs_ns_196gal	0.0288	0.0288	0.0143	0.0292	0.0308	0.0124
Kobs_ns_100gal	0.0238	0.0239	0.0120	0.0234	0.0236	0.0103

	Training case					
	Model C			Model D		
Testing case	1	2	6	1	2	6
El_ns_220gal	0.0432*	0.0430	0.0542	0.0424*	0.0434	0.0549
El_ns_196gal	0.0483	0.0479*	0.0603	0.0478	0.0479*	0.0606
El_ns_100gal	0.0526	0.0527	0.0650	0.0528	0.0525	0.0646
El_ns_50gal	0.0546	0.0549	0.0674	0.0551	0.0545	0.0670
El_ns_10gal	0.0552	0.0557	0.0681	0.0558	0.0551	0.0677
Kobs_ns_250gal	0.0279	0.0301	0.0216*	0.0293	0.0299	0.0175*
Kobs_ns_196gal	0.0289	0.0299	0.0232	0.0295	0.0307	0.0184
Kobs_ns_100gal	0.0239	0.0232	0.0196	0.0228	0.0236	0.0157

	Training case					
	Model E			Model F		
Testing case	1	2	6	1	2	6
El_ns_220gal	0.0412*	0.0619	0.0548	0.0398*	0.1263	0.0623
El_ns_196gal	0.0484	0.0468*	0.0609	0.0513	0.0470*	0.0704
El_ns_100gal	0.0528	0.0540	0.0647	0.0538	0.0539	0.0725
El_ns_50gal	0.0546	0.0562	0.0669	0.0558	0.0557	0.0750
El_ns_10gal	0.0552	0.0568	0.0676	0.0566	0.0562	0.0758
Kobs_ns_250gal	0.0299	0.0589	0.0161*	0.0517	0.0910	0.0183*
Kobs_ns_196gal	0.0294	0.0416	0.0177	0.0328	0.0368	0.0206
Kobs_ns_100gal	0.0238	0.0246	0.0158	0.0249	0.0247	0.0176

Note: * indicates the RMS error from different training case and others are the RMS error from prediction.

TABLE 10. RMS Error of Network Performance for Tested Steel Structure I/O Mapping

Testing case (1)	Training Case 1 (2)	2 (3)	3 (4)	4 (5)	5 (6)
(a) Model A					
Kobe × 20%	0.0985*	0.0992	0.0999	0.1020	0.1017
Kobe × 32%	0.0972	0.0965*	0.0978	0.0991	0.0996
Kobe × 40%	0.1087	0.1075	0.1049*	0.1064	0.1075
Kobe × 52%	0.1053	0.1009	0.0941	0.0923*	0.0945
Kobe × 60%	0.1245	0.1225	0.1190	0.1183	0.1164*
(b) Model B					
Kobe × 20%	0.0828*	0.0838	0.0848	0.0882	0.0886
Kobe × 32%	0.0805	0.0794*	0.0808	0.0833	0.0843
Kobe × 40%	0.0868	0.0851	0.0828*	0.0875	0.0880
Kobe × 52%	0.0863	0.0808	0.0776	0.0718*	0.0752
Kobe × 60%	0.1156	0.1120	0.1083	0.1062	0.1030*
(c) Model C					
Kobe × 20%	0.0618*	0.0781	0.0836	0.0929	0.0932
Kobe × 32%	0.1436	0.0590*	0.0976	0.0845	0.0911
Kobe × 40%	0.2889	0.1310	0.0545*	0.0881	0.1771
Kobe × 52%	0.4666	0.2459	0.2429	0.0527*	0.1207
Kobe × 60%	0.5166	0.2842	0.2848	0.1188	0.0794*

Note: * indicates RMS error from different training cases, and remaining values indicate RMS error from prediction.

TABLE 11. Identified I/O Mapping Model for Tested Steel Structure (x_i is ith Floor Acceleration)

Model (1)	Equation (2)
A (Linear)	$\ddot{x}_2(k) = \sum_{i=0}^{4} a_i \times \ddot{x}_1(k-i) + \sum_{j=0}^{4} b_j \times \ddot{x}_3(k-j)$
B (Linear)	$\ddot{x}_2(k) = \sum_{i=0}^{8} a_i \times \ddot{x}_1(k-i) + \sum_{j=0}^{8} b_j \times \ddot{x}_3(k-j)$
C (Nonlinear)	$\ddot{x}_2(k) = \sum_{m=1}^{5} w_m \times \left(\sum_{i=0}^{8} a_{im} \times \ddot{x}_1(k-i) + \sum_{j=0}^{8} b_{jm} \times \ddot{x}_3(k-j) \right)$

to determine the nonlinear model. Through numerical examples and shaking table test data of a steel frame structure, the discussion on time domain identification algorithm was made.

ACKNOWLEDGMENT

The writers gratefully acknowledge the support of the National Science Council (Taiwan) under grant No. NSC88-2211-E-002-006.

APPENDIX I. REFERENCES

Agbabian, M. S., Masri, S. F., Miller, R. K., and Caughey, T. K. (1991). ''System identification approach to detection of structural changes.'' *J. Engrg. Mech.*, ASCE, 117(2), 370–390.

Bendat, J. S., Palo, P. A., and Coppolino, R. N. (1992). ''A general identification technique for nonlinear differential equation of motion.'' *Probabilistic Engrg. Mech.*, 7, 43–61.

Billings, B. A., and Tsang, K. M. (1989). ''Spectral analysis for nonlinear system, part I: Parametric nonlinear spectral analysis.'' *Mech. Sys. and Signal Processings*, 3(4), 319–339.

Billings, S. A., Tsang, K. M., and Tomlinson, G. R. (1990). ''Spectral analysis for nonlinear systems, part III: Case study examples.'' *Mech. Sys. and Signal Processings*, 4(1), 3–21.

Caravani, P., Watson, M. L., and Thomson, W. T. (1977). ''Recursive least-square time domain identification of structural parameters.'' *J. Appl. Mech.*, ASME, 44(3), 135–150.

Chassiakos, A. G., and Masri, S. F. (1994). ''Adaptive identification of hysteretic structural systems.'' *Proc., 1st World Conf. on Structural Control*, Vol. 2, Pasadena, TP3:23–32.

Chen, S., and Billings, S. A. (1989). ''Representations of nonlinear systems: The NARMAX model.'' *Int. J. Control*, 49, 1013–1032.

Diaz, H., and Desrochers, A. A. (1988). ''Modeling of nonlinear discrete-time system from input-output data.'' *Automatica*, 24, 629–641.

Funahashi, K. (1989). ''On the approximate realization of continuous mapping by neural networks.'' *Neural Networks*, 2, 183–192.

Hoshiya, M., and Saito, E. (1984). ''Structural identification by extended Kalman filter.'' *J. Engrg. Mech.*, ASCE, 110(12), 1757–1770.

Huang, N. E., et al. (1998). ''The empirical mode decomposition and the Hilbert spectrum for nonlinear and non-stationary time series analysis.'' *Proc., Royal Soc.*, London, 454, 903–995.

Ioan, D. L. (1990). *System identification and control design*, Prentice-Hall, Englewood Cliffs, N.J.

Juang, J.-N. (1997). ''Unification of several system realization algorithm.'' *J. Guidance, Control, and Dyn.*, 74(1), 67–73.

Ljung, L., and Söderström, T. (1983). *Theory and practice of recursive identification*, MIT Press, Cambridge, Mass.

Loh, C. H., and Duh, J. Y. (1996). ''Analysis of nonlinear system using NARMA models.'' *J. Struct. Engrg. and Earthquake Engrg.*, Tokyo, 13(1), 11s–21s.

Loh, C. H., and Lin, H. M. (1996). ''Application of off-line and on-line identification techniques to building seismic response data.'' *Earthquake Engrg. and Struct. Dyn.*, 25, 269–290.

Masri, S. F., Nakamura, M., Chassiakos, A. G., and Caughey, T. K. (1996). ''Neural network approach to detection of changes in structural parameters.'' *J. Engrg. Mech.*, ASCE, 122(4), 350–360.

Masri, S. F., Sassi, H., and Caughey, T. K. (1982). ''Nonparametric identification of early arbitrary nonlinear system.'' *J. Appl. Mech.*, 49, 619–628.

Naike, H. G., and Yao, J. T. P. (1986). ''Research topics in structural identification.'' *Proc., 3rd Conf. on Dyn. Response of Struct.*, ASCE, New York, 542–550.

Naike, H. G., and Yao, J. T. P. (1988). ''System identification of approaches in structural safety evaluation.'' *Structural safety evaluation based on system identification approaches*, H. G. Naike and J. T. P. Yao, eds., Vieweg, Brunswick, Germany, 460–473.

Safac, E. (1989). ''Adaptive modeling, identification, and control of dynamic structural systems: I. Theory.'' *J. Engrg. Mech.*, ASCE, 115(11), 2386–2405.

Sato, T., and Qi, K. (1998). ''Adaptive H_∞ filter: Its application to structural identification.'' *J. Engrg. Mech.*, ASCE, 124(11), 1233–1240.

Sato, T., and Takei, K. (1997). ''Real time robust identification algorithm for structural systems with time-varying dynamic characteristics.'' *Proc., SPIE's 4th Annu. Symp. on Smart Struct. and Mat.*, SPIE, Bellingham, Wash.

Shinozuka, M., Yun, C. B., and Imai, H. (1982). ''Identification of linear structural dynamic systems.'' *J. Engrg. Mech. Div.*, ASCE, 108(6), 1371–1390.

Stry, G., and Moak, D. J. (1992). ''An experimental study of nonlinear dynamic system identification.'' *Nonlinear Dyn.*, (3), 1–11.

Xia, Q., Rao, M. Y., and Shen, X. (1994). ''Adaptive fading Kalman filter with an application.'' *Automatica*, 30, 1333–1338.

APPENDIX II. NOTATION

The following symbols are used in this paper:

$F[\ ]$ = nonlinear function of input $u(t)$ and output $y(t)$;
G_v = FRF;
H_v = Hilbert transform of FRF;
$\mathbf{P}^{-1}(t)$ = adaptation gain matrix;
$\mathbf{Q}_0$ = vector of unknown parameters;
$v_i(t)$ = horizontal displacement of ith floor;
$\ddot{x}_g(t)$ = input ground acceleration;
$y(t)$ = output measurement;
$\eta_i(x)$ = flexural type mode shape;
$\theta_i(t)$ = ith floor rotation;
$\lambda(k)$ = forgetting factor in discrete time k;
$\lambda(t)_i$ = weighting sequence (i = 1, 2); and
$\psi_i(x)$ = shear type mode shape.